e-Prime - Advances in Electrical Engineering, Electronics and Energy 9 (2024) 100687

Contents lists available at ScienceDirect

e-Prime - Advances in Electrical Engineering, Electronics and Energy

journal homepage: www.elsevier.com/locate/prime

Efficient voltage regulation: An RW-ARO optimized cascaded controller approach

Erdal Eker [a], Davut Izci [b,c], Serdar Ekinci [b], Hazem Migdady [d], Raed Abu Zitar [e], Laith Abualigah [f,g,h,i,j,*]

[a] Vocational School of Social Sciences, Muş Alparslan University, Muş 49250, Turkey
[b] Department of Computer Engineering, Batman University, Batman 72100, Turkey
[c] Applied Science Research Center, Applied Science Private University, Amman 11931, Jordan
[d] CSMIS Department, Oman College of Management and Technology, 320 Barka, Oman
[e] Faculty of Engineering and Computing, Liwa College, Abu Dhabi, United Arab Emirates
[f] Computer Science Department, Al al-Bayt University, Mafraq 25113, Jordan.
[g] MEU Research Unit, Middle East University, Amman 11831, Jordan.
[h] Jadara Research Center, Jadara University, Irbid 21110, Jordan
[i] Artificial Intelligence and Sensing Technologies (AIST) Research Center, University of Tabuk, Tabuk 71491, Saudi Arabia
[j] School of Engineering and Technology, Sunway University Malaysia, Petaling Jaya 27500, Malaysia

ARTICLE INFO

Keywords:
Artificial rabbits optimization algorithm
Random Walk strategy
Automatic voltage regulator
Cascaded RPIDD^2-PI controller
Optimization

ABSTRACT

This work introduces novel advancements in automatic voltage regulator (AVR) control, addressing key challenges and delivering innovative contributions. The primary motivation lies in enhancing AVR performance to ensure stable and reliable voltage output. A crucial innovation in this work is the introduction of the random walk aided artificial rabbits optimizer (RW-ARO). This novel optimization strategy incorporates a random walk approach, enhancing the efficiency of AVR control schemes. The proposed cascaded RPIDD^2-PI controller, fine-tuned using the RW-ARO, stands out as a pioneering approach in the AVR domain. It demonstrates superior stability, faster response times, enhanced robustness, and improved efficiency compared to existing methods. Comparative analyses with established controller approaches reaffirm the exceptional performance of the proposed method. The new approach results in shorter rise times, quicker settling times, and minimal overshoot, highlighting its effectiveness and speed in achieving desired system responses. Moreover, the novel approach attains higher phase and gain margins, showcasing its superior performance in the frequency domain. The disturbance rejection and harmonic analysis are performed in order to demonstrate the efficacy of the proposed approach for potential real-world applications. The latter analyses further cement the superior capability of the proposed approach for the automatic voltage regulation.

1. Introduction

Automatic voltage regulators (AVRs) play a vital role in the realm of electrical systems, ensuring a stable and reliable voltage output that is essential for optimal performance and the protection of equipment [1,2]. The efficacy of an AVR is dependent on its capacity to effectively control essential variables, such as voltage regulation, response time, stability, and efficiency [3]. Understanding of these factors is essential for guaranteeing a dependable and flexible power supply, even in the face of varying demands and input voltages [4–6]. As a result, the engineering community is devoted to exploring innovative avenues [7,8] to enhance AVR control methodologies [9–14].

The integration of a controller in conjunction with an AVR carries substantial significance for a variety of convincing rationales. To begin with, a controller serves as a centralized system that facilitates diligent monitoring and regulation of the AVR, hence improving the efficiency and effectiveness of voltage control. The controller serves as the central point for gathering essential data pertaining to voltage, frequency, and various other system factors, facilitating immediate modifications to uphold voltage stability. In addition, a controller integrates advanced features such as remote monitoring, defect detection, and automated shutdown in the event of emergencies, serving as a safeguard against

* Corresponding author.
E-mail address: aligah.2020@gmail.com (L. Abualigah).

https://doi.org/10.1016/j.prime.2024.100687
Received 2 November 2023; Received in revised form 1 July 2024; Accepted 10 July 2024
Available online 11 July 2024

equipment damage, minimizing operational disruptions, and ensuring the welfare of personnel. In essence, a controller enhances the dependability and effectiveness of the system through the provision of timely feedback and control over the AVR. This optimization enhances the efficiency of the generator or alternator, decreases energy consumption, and prolongs the lifespan of the equipment. Consequently, a range of controllers are utilized in this particular context, encompassing the conventional proportional-integral-derivative (PID) as well as PIDA, PIDD^2, RPID, FOPID, and FOPIDD^2. Each of these controllers offers unique features to cater to a wide range of AVR control needs [15–25].

In the existing literature, the standard PID controller is widely employed. It consists of three key components: the proportional (K_p), integral (K_i), and derivative (K_d) gains, combined to compute the control signal [26]. The promise of PID controller was demonstrated in a recent study reported in ref [27]. This study focuses on optimizing the AVR by employing PID controller and it utilizes integrated square error performance index together with exponential distribution and transit search optimizers for tuning the parameters. Comparative results with various techniques demonstrate superior stability, reduced steady-state error, and improved damping frequency, lowering oscillations and overshoot. Robustness testing further confirms the reliability and effectiveness of the proposed methods.

Despite the demonstrated efficacy of the classical PID controller, its more advanced versions have greater promise. For example, The RPID controller is a variation of the PID controller, introducing a modification to the derivative term with an additional filter coefficient, N, enhancing control flexibility [28]. FOPID controllers provide a more adaptable approach by introducing fractional orders (λ and μ) to the integral and derivative terms, allowing for customization based on the specific system's needs [29]. The PIDD^2 controller extends the PID controller by introducing a second-order derivative term, enhancing its capability to address specific system dynamics [30].

It is feasible to encounter different control structures such as the ones reported in [31–40]. All these controllers offer distinct advantages and characteristics, making them suitable for AVR control applications. However, in addition to control structures, the choice of a cost function significantly impacts performance [41]. Various cost functions are utilized by researchers, such as the integral of time-weighted squared error, integral of squared error, integral of absolute error, and integral of time-weighted absolute error. Additionally, the Zwe-Lee Gaing (ZLG) cost function, which is based on dynamic response performance criteria, is also employed [42–44].

Within a power system, the AVR serves a crucial function in the preservation of voltage stability, hence guaranteeing that interconnected electrical apparatus functions within acceptable voltage thresholds [45–49]. Inadequate voltage control can result in significant repercussions, such as harm to equipment, operational malfunctions, expensive periods of inactivity, and the requirement for major repairs. Therefore, the AVR plays a crucial role in power systems that depend on generators or alternators to produce energy. Although current control approaches have demonstrated some degree of success, they are not without their limits [50]. Challenges related to robustness, relatively higher overshoots, prolonged rise, settling, and peak times, as well as persistent steady-state errors, persist in these existing control approaches. These challenges underscore the motivation for our study. The primary motivation behind this research is to propose an advanced control scheme that can effectively address the aforementioned limitations. Furthermore, as part of our motivation, we have developed a novel optimizer based on the artificial rabbits optimizer (ARO) [51] to fine-tune the parameters of our proposed control scheme, improving its overall performance and adaptability. The objective of these endeavors is to expand the limits of AVR control and provide a valuable contribution to the advancement of power systems that are more resilient and effective.

In line with the motivations presented above, we introduce a novel cascaded RPIDD^2-PI controller as an innovative alternative to existing controller types. The purpose of this setup is to provide improved accuracy, stability, and responsiveness in voltage control, thereby addressing the constraints commonly associated with traditional approaches. Furthermore, we have developed an enhanced ARO (RW-ARO) algorithm, integral to the motivation of this work. The original ARO technique utilizes an iterative procedure in which rabbits can randomly choose burrows. This method accelerates the process of reaching a consensus, but it may inadvertently diminish the variety of possible alternatives. To address these challenges, we integrated a random walk (RW) strategy for enhanced explorative performance [52]. In this regard, the presented methodology in this study is different that of the one presented in ref [21], which has also been used to improve the structure of the original ARO. The improvement approach presented in ref [21] employs adaptive local search (ALS) and experience-based perturbed learning (EPL) mechanisms. In contrast, in this study, the innovation lies in enhancing the exploration capability of the ARO algorithm through the introduction of a random walk mechanism for the first time. The optimization algorithm employed in this study refines the parameters of the control scheme suggested, resulting in enhanced performance and flexibility. Utilizing the ZLG cost function [53] for the purpose of minimization has several benefits. The aforementioned methodology effectively mitigates the performance metrics associated with dynamic response, such as maximum overshoot, steady-state error, settling time, and rising time. Consequently, the AVR system is able to meet rigorous performance standards [54]. Significantly, this work is the first publication on the application of such a methodology for AVR systems.

The main objective of this study is to showcase the enhanced effectiveness of the cascaded RPIDD^2-PI controller, which has been optimized using the innovative RW-ARO algorithm, in tackling the aforementioned difficulties associated with AVR control. The goal is to outperform other documented AVR control methods in terms of stability, response speed, resilience, and effectiveness. To verify the superiority of the proposed RW-ARO algorithm, the stability of the cascaded RPIDD^2-PI controller was assessed by employing the original ARO [51], differential evolution [55], gravitational search algorithm [56] and particle swarm optimization [57]. The results indicated that the RW-ARO algorithm consistently achieved the lowest average fitness value with accuracy. Additionally, the convergence profile analysis demonstrated that RW-ARO achieved a lower objective function value in fewer iterations while maintaining the lowest value through continuous iterations compared to the other algorithms. The RW-ARO-tuned system also exhibited the fastest rise time, the shortest settling time, and minimal overshoot, indicating a highly stable and well-tuned control system. Moreover, the RW-ARO provided a higher phase margin and gain margin compared to the other algorithms, signifying enhanced performance and improved stability. Superiority verification in terms of disturbance rejection and harmonic analysis further confirm the effectiveness of the proposed approach.

We conducted a comparative analysis between the suggested RW-ARO-based cascaded PIDD^2-PI controller system and many other well-established controller approaches documented in the literature to evaluate its efficacy. These included the tree seed optimization based PID controller [58], symbiotic organism search optimization based PID with filter controller [59], slime mould optimization based FOPID controller [60], teaching learned optimization based PIDA controller [61] and improved Lévy flight distribution algorithm with fitness distance balance based PIDD^2 controller [62]. The comparative responses revealed that the proposed approach outperformed other methods in terms of shorter rise times, settling times, and minimal overshoot, highlighting its effectiveness and speed in achieving desired system responses. The comparative Bode plots illustrated that the proposed approach achieved a higher phase margin and gain margin compared to the other methods, signifying its robustness and superior performance in the frequency domain. Further performance evaluation against the other reported approaches [31–40] confirmed the efficacy of the proposed

approach for the automatic voltage regulation. Besides, the external disturbance rejection and the total harmonic distortion analyses were performed to demonstrate the better convenience of the proposed approach in terms of real conditions that may be encountered in real-world.

2. Artificial Rabbits Optimizer

The ARO is a recently developed metaheuristic approach, drawing inspiration from the survival strategies of rabbit populations [51]. The objective of this algorithm is to simulate the complex behaviors exhibited by rabbits, with a specific focus on their employment of random concealment and detour foraging strategies. In this algorithm, a population of virtual rabbits forms a collective, with each member being responsible for a designated eating zone teeming with vegetation and burrows. While foraging, these virtual rabbits embark on a serendipitous exploration of burrows belonging to their peers in search of sustenance. This process encompasses not only the collection of food resources but also introduces a certain level of unpredictability into their actions, achieved by updating their positions based on interactions with fellow rabbits. This intricate foraging behavior can be expressed mathematically as follows:

$$\vec{\Delta}_i(t+1) = \vec{z}_j(t) + \rho.\left(\vec{z}_i(t) - \vec{z}_j(t)\right) + round(0.5\ .(0.05+g_1)).n_1, i, j = 1, 2\ldots\ldots, M \text{ and } i \neq j \tag{1}$$

$$E = \left(e - e^{\left(\frac{1-t}{T}\right)^2}\right).\sin(2\pi g_2) \tag{2}$$

$$c(k) = \begin{cases} 1 & if\ k == h(u) \\ 0 & else \end{cases},\ k = 1, \ldots, d\ \&\ u = 1, 2, \ldots, \lceil g_3.d \rceil \tag{3}$$

where $\rho = E.c$, $h = randperm(d)$, n_1 follows a normal distribution, and g_1, g_2 and g_3 represent uniform random numbers within the interval [0, 1]. $\vec{z}_i(t)$, $\vec{\Delta}_i(t+1)$, M, T, d, $round$, $randperm$, and E identify the present location of i^{th} candidate at time t, i^{th} updated candidate at time $t+1$, the population size of rabbits, the final number of repetitions, the problem size the rounding process to the closest integer value, a random permutation function encompassing values from 1 to the problem size and the total time of the foraging round, respectively. During the phase of exploitation, rabbits utilize a strategic approach of random concealment in order to elude predators, wherein they construct burrows in close

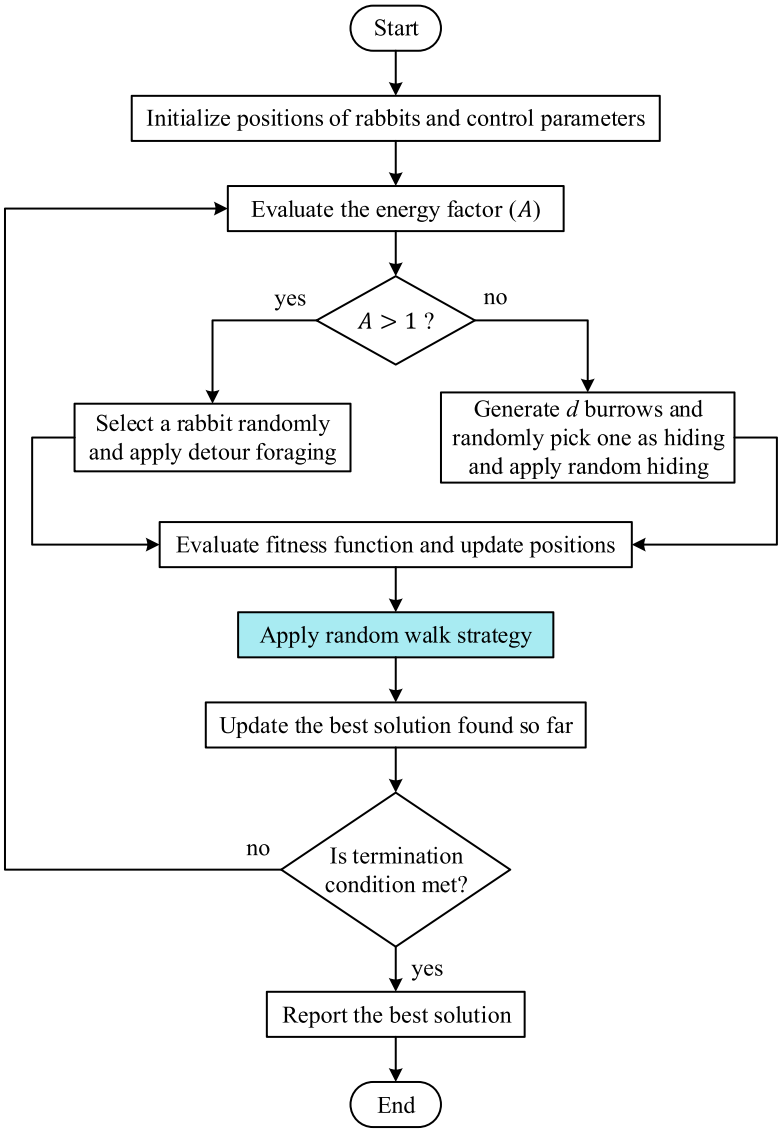

Fig. 1. Flowchart of RW-ARO.

proximity to their initial positions. During each cycle, a rabbit produces b burrows in each dimension and chooses one to seek shelter. Mathematically, this process can be expressed as:

$$\vec{BU_{ij}}(t) = \vec{z_i}(t) + H.h.\vec{z_i}(t), i = 1, 2\ldots\ldots, M \text{ and } j = 1, 2\ldots\ldots, d \quad (4)$$

$$H = \frac{1 - t + T}{T} g_4 \quad (5)$$

$$h(k) = \begin{cases} 1 & \text{if } k == j \\ 0 & \text{else} \end{cases}, \; k = 1, \ldots, d \quad (6)$$

Here, $n_2 \sim N(0, 1)$, H represents the hiding function, and d is the number of formed burrows within the rabbit's area. The size of the neighborhood where burrows are generated shrinks as the number of iterations increases. In the random hiding mode, the rabbit's position is updated as follows:

$$\vec{\Delta}_i(t+1) = \vec{z_i}(t) + \rho.\left(g_4.BU_{ir}(t) - \vec{z_i}(t)\right), \; i = 1, 2, \ldots\ldots M \quad (7)$$

$$h_r(k) = \begin{cases} 1 & \text{if } k == \lceil g_5.d \rceil \\ 0 & \text{else} \end{cases}, \; k = 1, \ldots, d \quad (8)$$

$$BU_{ir}(t) = \vec{z_i}(t) + H.h_r.\vec{z_i}(t) \quad (9)$$

In this context, $BU_{ir}(t)$ indicates the burrow selected by the rabbit during the concealment phase, and g_4 and g_5 denote random values falling within the [0,1] range. The position of the rabbit is subject to updates through either a detour foraging mode or a randomized hiding process, as described in the following manner.

$$\vec{z_s}(t+1) = \begin{cases} \neg z_s(t) & f(\neg z_s(t)) \le f(\neg \Delta_s(t+1)) \\ \neg \Delta_s(t+1) & f(\neg z_s(t)) > f(\neg \Delta_s(t+1)) \end{cases} \quad (10)$$

Should the fitness of the s^{th} rabbit's candidate surpass the fitness of its present position, the rabbit relocates to the candidate's location, determined by either Eq. (1) or Eq. (7). Rabbit energy diminishes as iterations advance, facilitating the shift from an exploratory phase to an exploitative one, characterized as follows:

$$A(t) = 4\left(1 - \frac{t}{T}\right) ln\left(\frac{1}{\alpha}\right) \quad (11)$$

where α represents a random number. When $A(t) > 1$, the algorithm focuses on global search (exploration), and when $A(t) \le 1$, it focuses on local search (exploitation).

3. Random Walk ARO Algorithm

The random walk artificial rabbits optimization (RW-ARO) algorithm leverages the concept of random walk [63], which is a stochastic process characterized by consecutive random steps. In mathematical terms, a random walk (RW) can be expressed as follows [64].

$$W_N = \sum_{i=1}^{N} S_i \quad (12)$$

Here, W_N represents the final state after N random steps, and S_i signifies each individual random step taken from a specific distribution. The crucial aspect of a random walk is that the next state (W_N) solely depends on the current state (W_{N-1}) and the step taken from the current state to the next state (S_N). The step size, s_i, can either be fixed or vary in each iteration. This variability is controlled by a parameter α_i, where $\alpha_i > 0$. Essentially, for a "rabbit" starting from a point x_0 and ending at x_n, the random walk can be defined as a summation of these steps, as shown in the equation below:

$$x_n = x_0 + \alpha_1 s_1 + \alpha_2 s_2 + \ldots + \alpha_N s_N = x_0 + \sum_{i=1}^{N} \alpha_i S_i \quad (13)$$

Table 1
Statistical results on unimodal functions.

Function (Name/Global Optimum)	Statistical metric	ARO	RW-ARO
BF1 ("Sphere"/0)	Average	1.0558E−31	**6.2215E−34**
	Standard deviation	5.7343E−31	**2.3148E−33**
	Minimum	8.1192E−41	**1.2169E−42**
	Maximum	3.1417E−30	**1.2398E−32**
BF2 ("Schwefel 2.2"/0)	Average	2.1257E−19	**1.2112E−19**
	Standard deviation	5.8767E−19	**2.5143E−19**
	Minimum	2.5847E−23	**6.5891E−24**
	Maximum	3.0268E−18	**1.0189E−18**
BF3 ("Schwefel 1.2"/0)	Average	2.0920E−22	**4.4928E−24**
	Standard deviation	1.1152E−21	**1.5680E−23**
	Minimum	3.2710E−33	**2.1775E−35**
	Maximum	6.1126E−21	**8.4084E−23**
BF4 ("Schwefel 2.21"/0)	Average	6.1879E−14	**9.3145E−15**
	Standard deviation	2.7366E−13	**2.3281E−14**
	Minimum	1.3534E−17	**1.3533E−17**
	Maximum	1.5050E−12	**1.1621E−13**
BF5 ("Rosenbrock"/0)	Average	1.4640E+00	**9.9950E−01**
	Standard deviation	2.5371E+00	**1.2516E+00**
	Minimum	7.0600E−02	**1.2700E−02**
	Maximum	1.1210E+01	**4.3556E+00**
BF6 ("Step"/0)	Average	**0**	**0**
	Standard deviation	**0**	**0**
	Minimum	**0**	**0**
	Maximum	**0**	**0**
BF7 ("Quartic"/0)	Average	9.9374E−04	**8.8510E−04**
	Standard deviation	**5.5624E−04**	5.6936E−04
	Minimum	1.7418E−04	**5.2610E−05**
	Maximum	2.6215E−03	**2.6000E−03**

The parameter α_i dictates the step size, and this allows the random walk to be utilized within various search algorithms. It serves the purpose of perturbing the population of solutions, preventing them from getting trapped in local optima. The choice of the step size distribution is a critical factor in the search process. A small step size encourages exploitation of the search space in the vicinity of the current state, focusing on fine-tuning existing solutions. In contrast, a sufficiently large step size promotes exploration of uncharted territories within the search space, potentially unveiling new and promising regions to explore. In line with this strategy, the RW-ARO algorithm was developed as an enhancement to the original ARO approach. Its goal is to improve the search process (exploration) and the quality of solutions achieved. In the context of an AVR system, this algorithm ensures that the AVR system operates efficiently by optimizing its parameters and responses. In the RW-ARO algorithm, the original ARO algorithm is performed as a foundation, and then further improvements are achieved through the incorporation of a random walk mechanism as outlined in the flowchart given in Fig. 1. This random walk strategy helps diversify the solutions and avoid convergence to local optima, ultimately leading to better and more effective control of the AVR system. The RW-ARO algorithm's application in the AVR system demonstrates its efficacy in fine-tuning and optimizing system parameters to maintain voltage regulation and stability, making it a valuable tool in the field of control systems. Besides, the developed RW-ARO algorithm is more preferrable in the proposed design approach for the AVR as it does not require additional parameter tuning beyond population size and total iteration number.

4. Experimental results on twenty-three benchmark functions

The performance of ARO and RW-ARO was assessed in our study, encompassing a wide range of twenty-three benchmark functions. These

Table 2
Statistical results on multimodal benchmark functios.

Function (Name/Global Optimum)	Statistical metric	ARO	RW-ARO
BF8 ("Schwefel"/ −1.2569E+04)	Average	−9.9154E+03	**−9.9384E+03**
	Standard deviation	**4.3461E+02**	4.9039E+02
	Minimum	−1.0768E+04	**−1.0905E+04**
	Maximum	−8.9888E+03	**−9.0812E+03**
BF9 ("Rastrigin"/0)	Average	**0**	**0**
	Standard deviation	**0**	**0**
	Minimum	**0**	**0**
	Maximum	**0**	**0**
BF10 ("Ackley"/0)	Average	1.1250E−15	**8.8818E−16**
	Standard deviation	9.0135E−16	**1.0029E−31**
	Minimum	8.8818E−16	**8.8818E−16**
	Maximum	4.4409E−15	**8.8818E−16**
BF11 ("Griewank"/0)	Average	**0**	**0**
	Standard deviation	**0**	**0**
	Minimum	**0**	**0**
	Maximum	**0**	**0**
BF12 ("Penalized"/0)	Average	4.2465E−03	**9.7430E−04**
	Standard deviation	1.9051E−02	**1.4000E−03**
	Minimum	1.3022E−04	**5.8094E−05**
	Maximum	1.0496E−01	**6.8000E−03**
BF13 ("Penalized2"/0)	Average	8.0105E−03	**5.4336E−03**
	Standard deviation	8.0093E−03	**5.1455E−03**
	Minimum	5.6591E−04	**3.4087E−04**
	Maximum	2.7334E−02	**1.8562E−02**

functions are categorized into three groups: unimodal, multimodal, and low-dimensional, and we conducted 30 runs for each with a population size of 40 and a total of 300 iterations.

Table 1 presents the statistical results for unimodal benchmark functions (BF1 to BF7). It is evident that RW-ARO consistently outperforms ARO across all these functions. RW-ARO achieves lower average fitness values, smaller standard deviations, and superior minimum and maximum fitness values. Notably, in BF1 ("Sphere"), RW-ARO reaches an astonishing minimum fitness value of 1.2169E−42, significantly better than ARO's 8.1192E−41.

Table 2 provides clear evidence of the superior performance of RW-ARO in relation to the multimodal benchmark functions (BF8 to BF13). It consistently provides more accurate results with lower average fitness values, narrower standard deviations, and improved minimum and maximum fitness values. In BF10 ("Ackley"), RW-ARO achieves a maximum fitness value of 8.8818E−16, whereas ARO reaches 4.4409E−15, showcasing the precision of RW-ARO.

The results for low-dimensional benchmark functions (BF14 to BF23) are presented in Table 3. RW-ARO continues to exhibit superior performance. It maintains the precision and consistency that we observed in the previous categories. For example, in BF20 ("Hartman 6"), RW-ARO outperforms ARO in terms of both average and minimum fitness values.

5. AVR System

An AVR is a vital device utilized in power systems to control and stabilize the output voltage of a generator. Its primary function is to ensure a consistent output voltage, regardless of fluctuations in the load or input voltage, as described in [3]. The AVR operates by receiving signals from the generator's output voltage (V_t), comparing them to a reference voltage (V_{ref}), and adjusting the field current of the alternator to maintain a steady output voltage. To achieve this control, the AVR typically employs electronic components such as amplifiers, exciters, generators, and sensors, as depicted in the block diagram shown in Fig. 2 [42].

Table 3
Statistical results on low-dimensional benchmark functions.

Function (Name/Global Optimum)	Statistical metric	ARO	RW-ARO
BF14 ("Foxholes"/0.998)	Average	**9.9800E−01**	**9.9800E−01**
	Standard deviation	**3.3876E−16**	**3.3876E−16**
	Minimum	**9.9800E−01**	**9.9800E−01**
	Maximum	**9.9800E−01**	**9.9800E−01**
BF15 ("Kowalik"/ 3.0749E−04)	Average	3.2383E−04	**3.1013E−04**
	Standard deviation	5.7098E−05	**6.9340E−06**
	Minimum	3.0749E−04	**3.0749E−04**
	Maximum	6.2191E−04	**3.4243E−04**
BF16 ("Six-Hump Camel"/ −1.0316)	Average	−1.0316E+00	**−1.0316E+00**
	Standard deviation	1.8278E−15	**0**
	Minimum	−1.0316E+00	**−1.0316E+00**
	Maximum	−1.0316E+00	**−1.0316E+00**
BF17 ("Branin"/0.39789)	Average	**3.9790E−01**	**3.9790E−01**
	Standard deviation	1.8266E−12	**1.7964E−13**
	Minimum	**3.9790E−01**	**3.9790E−01**
	Maximum	**3.9790E−01**	**3.9790E−01**
BF18 ("Goldstein-Price"/ 3)	Average	**3.0000E+00**	**3.0000E+00**
	Standard deviation	**4.5168E−16**	**4.5168E−16**
	Minimum	**3.0000E+00**	**3.0000E+00**
	Maximum	**3.0000E+00**	**3.0000E+00**
BF19 ("Hartman 3"/ −3.8628)	Average	**−3.8628E+00**	**−3.8628E+00**
	Standard deviation	**2.7101E−15**	**2.7101E−15**
	Minimum	**−3.8628E+00**	**−3.8628E+00**
	Maximum	**−3.8628E+00**	**−3.8628E+00**
BF20 ("Hartman 6"/ −3.322)	Average	−3.2863E+00	**−3.3061E+00**
	Standard deviation	5.5401E−02	**4.1100E−02**
	Minimum	**−3.3220E+00**	**−3.3220E+00**
	Maximum	**−3.2031E+00**	**−3.2031E+00**
BF21 ("Shekel 5"/ −10.1532)	Average	−9.8999E+00	**−1.0150E+01**
	Standard deviation	1.3730E+00	**1.6300E−02**
	Minimum	**−1.0153E+01**	**−1.0153E+01**
	Maximum	−2.6304E+00	**−1.0064E+01**
BF22 ("Shekel 7"/ −10.4029)	Average	−1.0003E+01	**−1.0395E+01**
	Standard deviation	1.5319E+00	**1.4199E−09**
	Minimum	**−1.0403E+01**	**−1.0403E+01**
	Maximum	−3.7243E+00	**−1.0403E+01**
BF23 ("Shekel 10"/ −10.5364)	Average	−1.0313E+01	**−1.0536E+01**
	Standard deviation	1.2234E+00	**3.2242E−05**
	Minimum	**−1.0536E+01**	**−1.0536E+01**
	Maximum	−3.8354E+00	**−1.0536E+01**

The AVR is a crucial component in a power system since it is responsible for maintaining voltage stability and ensuring that electrical equipment linked to the system operates within acceptable voltage thresholds. However, effective control is crucial to achieve this objective. Figs. 3 and 4 provide insights into the step response and Bode plot of an uncontrolled AVR system, respectively. These figures reveal that the system's response exhibits pronounced oscillations, highlighting the need for regulation. Given the high voltage levels in power systems, these oscillations pose significant risks. Without proper voltage regulation, electrical equipment may be at risk of damage or operational failure, resulting in costly downtime and repairs.

6. Proposed RW-ARO-based design method

In AVR related studies, extended version standard PID controller known as PID plus second order derivative (PIDD^2) has so far been reported [30]. By introducing a second-order derivative term, the PIDD^2 controller effectively improves the system's phase margin, minimizes steady-state error, and enhances overall stability. However, it's

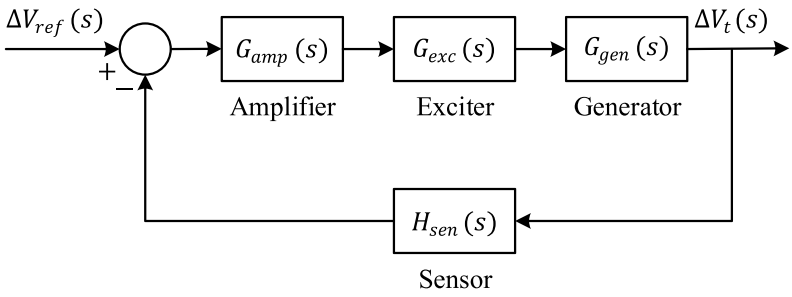

Fig. 2. Block diagram of an uncontrolled AVR system.

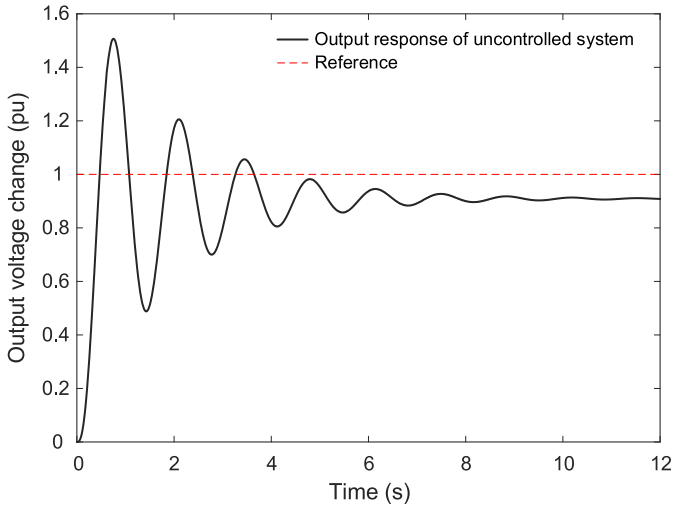

Fig. 3. Step response of an uncontrolled AVR system.

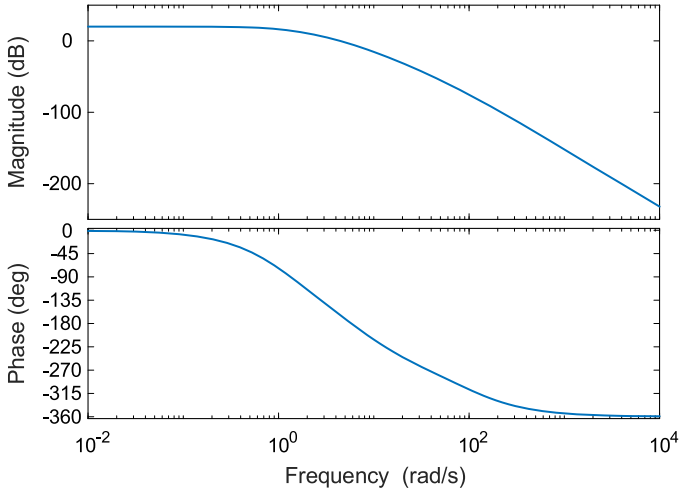

Fig. 4. Bode plot of an uncontrolled AVR system.

important to note that the additional derivative term in this controller may not be effective in high-frequency domains. This is due to the risk of amplifying control signals with sensor noise, which can negatively impact performance. To mitigate this issue, a low-pass filter can be added to the derivative term which is known as real PIDD^2 (RPIDD^2) controller [65].

In order to further increase the performance of the controller, we have also adopted a PI controller in a cascaded manner, resulting in the transfer function of the cascaded real PIDD^2 controller as shown in Eq. (14):

$$C_{PIDD^2-PI}(s) = \left[K_{p1} + \frac{K_{i1}}{s} + K_{d1}\frac{N_1 s}{s+N_1} + K_{d2}\left(\frac{N_2 s}{s+N_2}\right)^2\right] \times \left(K_{p2} + \frac{K_{i2}}{s}\right) \tag{14}$$

where K_{p1}, K_{i1}, K_{d1}, and K_{d2} denote proportional, integral, derivative, and second-order derivative gains, respectively. N_1 and N_2 represent the filter coefficients. Besides, K_{p2} and K_{i2} are proportional and integral gains of the employed PI controller, respectively. In light of this expression, Fig. 5 illustrates the block diagram of the proposed cascaded real PIDD^2-PI controller.

In this study, the following F cost function [42,53] has been employed for minimization as it can effectively minimize the dynamic response performance criteria such as percentage maximum overshoot (M_p), steady-state error (E_{ss}), settling time (S_t) and rise time (R_t) [54]. To reach a good performance, the balancing coefficient, ρ, has been set to 1. This coefficient is used for the optimal selection of performance metrics such as rise time, settling time, overshoot, and steady-state error, which are among the most important stability criteria of a system. Although the value of this coefficient varies, it is generally taken as 1 in literature [41, 66–68].

$$F = \rho \times (S_t - R_t) + (1-\rho) \times (M_p + E_{ss}) \tag{15}$$

For the minimization of F cost function, the limits of the parameters of cascaded real PIDD^2-PI controller have been chosen as $10^{-3} \leq K_{p1}, K_{i1}, K_{d1}, K_{p2}, K_{i2}, K_{d2} \leq 4$ and $100 \leq N_1, N_2 \leq 2000$. Through detailed and extensive analyses, it has been deemed appropriate to select the controller parameters within these limits. If the specified limits are exceeded, significant impacts on the stability performance of the controller would occur.

Fig. 6 shows the implementation of the RW-ARO to the AVR system controlled by the cascaded RPIDD^2-PI controllers. The related Fig. also provides the transfer functions of the respective AVR components (amplifier, exciter, generator and sensor) [69–72]. As depicted in the latter figure, the RW-ARO optimizes the controller parameters through the iterations by evaluating the F cost function. In this way, it achieves the best controller parameters for the AVR system.

7. Comparative simulation results on AVR system

7.1. Superiority verification of the RW-ARO over other competitive optimizers

To verify the superiority of the proposed RW-ARO algorithm, the stability of the cascaded real PIDD^2-PI controller has been assessed by employing the original ARO [51], differential evolution (DE) [55], gravitational search algorithm (GSA) [56] and particle swarm optimization (PSO) [57]. The population size, total number of iterations and number of runs have been selected as 40, 50 and 30, respectively.

Table 4 presents numerical results for comparative assessment of the statistical performance of the algorithms. The results in Table 4 indicate

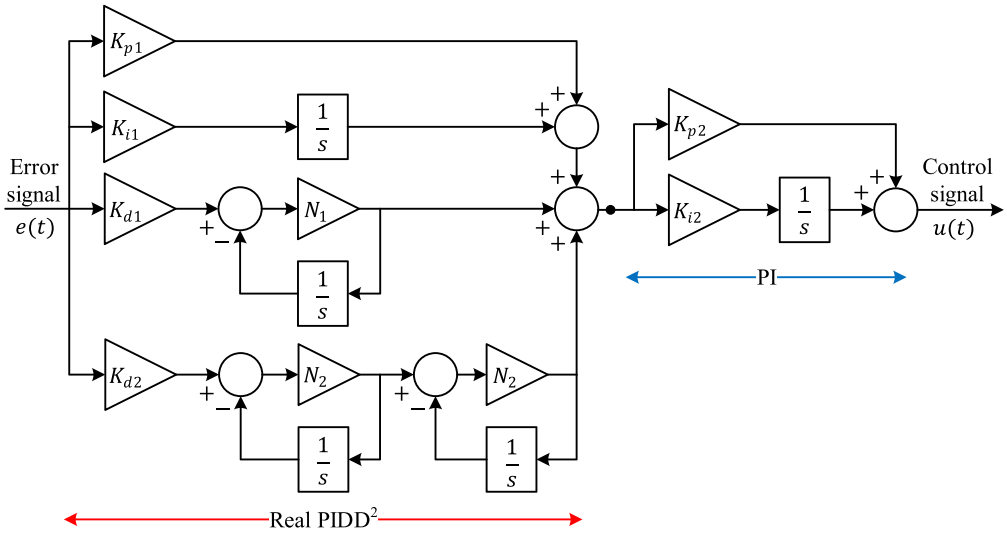

Fig. 5. Block diagram of proposed cascaded real PIDD^2-PI controller.

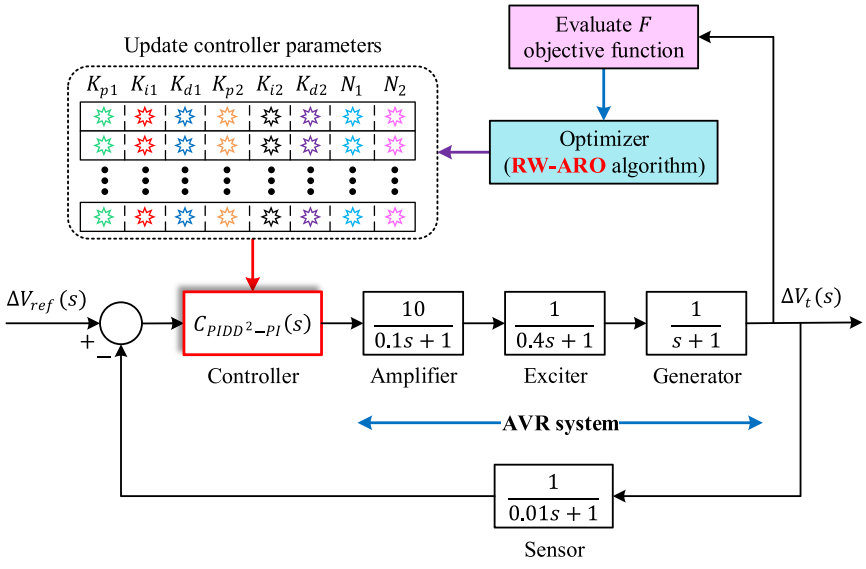

Fig. 6. Detailed block diagram of proposed novel approach.

Table 4
Statistical performance comparison for AVR system

Statistical metric	RW-ARO	ARO	DE	GSA	PSO
Average	**6.0415E−03**	7.1301E−03	8.3352E−03	7.5815E−03	8.8660E−03
Standard deviation	**9.0497E−05**	1.3273E−04	1.0649E−04	1.1249E−04	1.1615E−04
Minimum	**5.8973E−03**	6.9547E−03	8.1730E−03	7.4272E−03	8.7000E−03
Maximum	**6.2222E−03**	7.4853E−03	8.6127E−03	7.8268E−03	9.1463E−03

that the RW-ARO algorithm outperforms the other optimization algorithms. It achieves the lowest average fitness value (6.0415E−03) among all algorithms, which is notably better than ARO, DE, GSA, and PSO. The standard deviation for RW-ARO is also the smallest (9.0497E−05), highlighting its consistency and accuracy. Furthermore, RW-ARO reaches the lowest minimum fitness value (5.8973E−03) and maintains a competitive maximum fitness value (6.2222E−03).

In Fig. 7, we can observe the convergence behavior of the algorithms. RW-ARO stands out by achieving a lower objective function value in fewer iterations compared to the other algorithms. It not only converges faster but also maintains the lowest value through continuous iterations, indicating its efficiency in finding optimal solutions.

Table 5 displays the obtained controller parameters via RW-ARO, ARO, DE, GSA and PSO algorithms. With the adoption of those parameters, the comparative responses presented in Figs. 8 and 9 can be obtained for employed algorithms. Fig. 8 illustrates the comparative step responses for the AVR systems tuned by the different algorithms. It is evident that the RW-ARO-tuned system exhibits the fastest rise time, the shortest settling time, and minimal overshoot among all the systems. This indicates that RW-ARO not only converges quickly but also provides a highly stable and well-tuned control system. In Fig. 9, the Bode plots for the open-loop AVR systems reveal that RW-ARO provides a

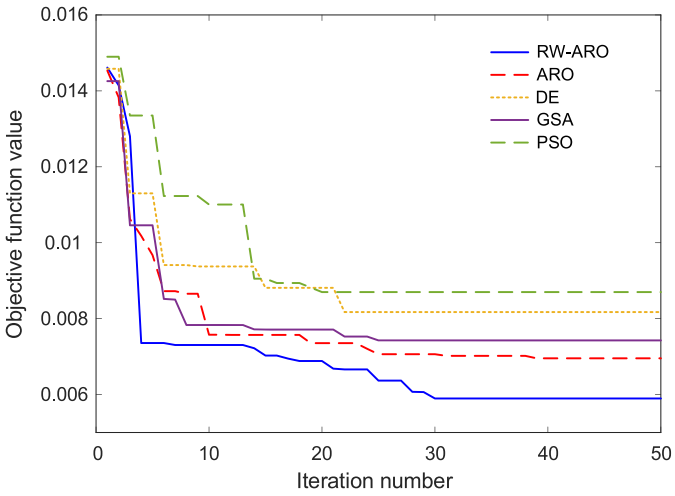

Fig. 7. Convergence evolutions of RW-ARO, ARO, DE, GSA and PSO algorithms.

Table 5
Obtained controller parameters via RW-ARO, ARO, DE, GSA and PSO.

Controller parameter	RW-ARO	ARO	DE	GSA	PSO
K_{p1}	3.8975	3.9716	3.8570	3.4083	3.2206
K_{i1}	0.65239	1.3686	1.6342	1.4468	0.85335
K_{d1}	1.4213	1.7505	1.9765	1.2922	1.7663
K_{p2}	1.2530	0.95493	0.80180	1.3570	0.98144
K_{i2}	0.30956	0.2633	0.30084	0.057177	0.29219
K_{d2}	0.12524	0.14375	0.15255	0.10611	0.13404
N_1	1887.8	1879.7	1921.8	1143.6	987.64
N_2	1975.1	981.98	839.57	1236.2	1730.8

higher phase margin and gain margin compared to the other algorithms. This signifies that the RW-ARO-tuned system is more robust and exhibits better control performance, with improved stability and robustness in the frequency domain. The related illustrations are numerically supported with the data presented in Table 6.

7.2. Superiority verification of the proposed approach over other effective approaches

To assess the effectiveness of the proposed RW-ARO/PIDD^2-PI controller approach, we conducted a comparative analysis with various other well-established controller methodologies documented in the literature. These approaches include tree seed algorithm (TSA) based PID controller [58], symbiotic organism search (SOS) algorithm-based PID with filter (PID-F) controller [59], slime mould algorithm (SMA) based fractional order PID (FOPID) controller [60], teaching learned optimization (TLBO) based PID acceleration (PIDA) controller [61] and improved Lévy flight distribution algorithm with fitness distance balance (FDB-LFD) based PIDD^2 controller [62].

In Fig. 10, we observe the comparative step responses for the RW-ARO/PIDD^2-PI controller approach and the other recent reported approaches. It is evident that the RW-ARO/PIDD^2-PI approach outperforms the other methods with the shortest rise time, settling time, and minimal overshoot. This demonstrates the effectiveness and speed of the proposed controller approach in achieving desired system responses.

Fig. 11 presents the comparative Bode plots for the RW-ARO/PIDD^2-PI controller approach and the other recent reported approaches. These plots reveal that the RW-ARO/PIDD^2-PI approach achieves a higher phase margin and gain margin compared to the other methods. This signifies its robustness and superior performance in the frequency domain, highlighting its ability to provide stable and accurate control over a wide range of frequencies.

The numerical results in Table 7 provide clear evidence of the superiority of the RW-ARO/PIDD^2-PI approach over the other controllers in terms of various stability metrics. The RW-ARO/PIDD^2-PI controller exhibits the shortest rise time (0.0318 seconds) among all the controllers, showcasing its ability to reach the desired setpoint rapidly. In comparison, most other controllers require considerably more time to achieve the same response. It also excels in settling time (0.0478 seconds), outperforming all other controllers. It quickly settles to a stable state, indicating its efficiency in reducing oscillations and ensuring system stability. Remarkably, the RW-ARO/PIDD^2-PI controller achieves zero overshoot, signifying that it can maintain system response without any initial transitory deviation. In contrast, some other controllers exhibit significant overshoot, indicating less effective control.

The proposed approach also offers a substantial phase margin (70.6399 degrees), indicating its robustness and ability to handle disturbances and variations. This surpasses most other controllers, which have smaller phase margins. It also boasts a notably higher gain margin (28.5713 dB) compared to other controllers. A higher gain margin suggests better stability and resilience against changes in the system's characteristics. The RW-ARO/PIDD^2-PI controller exhibits a broader bandwidth (68.3194 rad/s), enabling it to effectively control the system

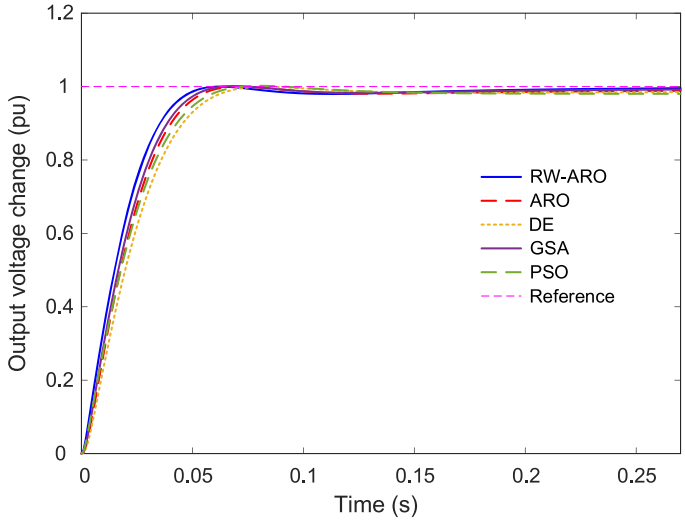

Fig. 8. Comparative step responses for RW-ARO, ARO, DE, GSA and PSO tuned AVR system.

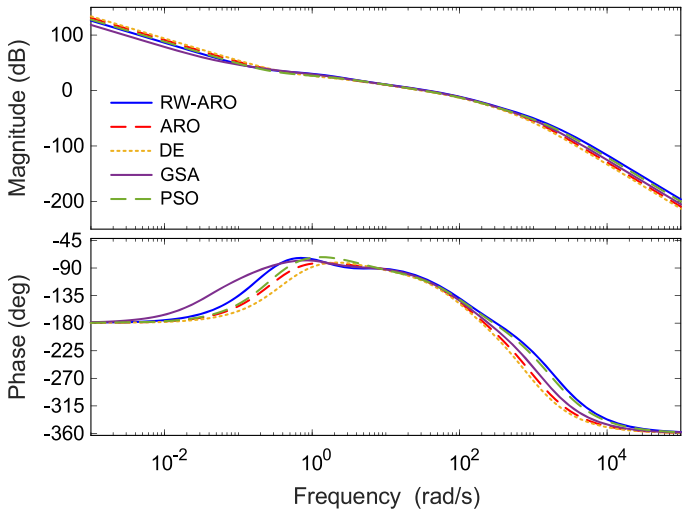

Fig. 9. Comparative Bode plots for RW-ARO, ARO, DE, GSA and PSO tuned open-loop AVR systems.

Table 6
Time and frequency domains based comparative results.

Stability metric	RW-ARO	ARO	DE	GSA	PSO
Rise time (s)	**0.0318**	0.0355	0.0402	0.0343	0.0388
Settling time (s)	**0.0478**	0.0544	0.0624	0.0519	0.0588
Overshoot (%)	**0**	**0**	**0**	0.1464	0.2109
Phase margin (°)	**70.6399**	69.9419	70.0744	70.1472	70.5673
Gain margin (dB)	28.5713	23.9044	23.5564	25.4066	**28.8856**
Bandwidth (rad/s)	**68.3194**	61.0391	53.7273	63.1620	55.3019

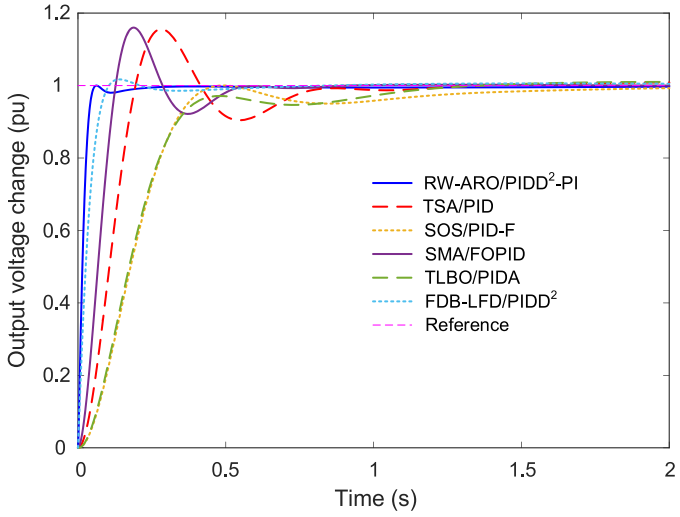

Fig. 10. Comparative step responses for RW-ARO/PIDD^2-PI and other recent reported approaches.

over a wide range of frequencies. This is an advantage, particularly in systems with varying dynamics.

Further performance comparisons were also considered in this study in order to better demonstrate the efficacy of the proposed approach from a wider perspective. In this regard, the reported works in refs. [31–40] were also considered. In Table 8, the comparative time domain performance analysis against reported works in the literature showcases the efficacy of the proposed RW-ARO/PIDD^2-PI in terms of rise time, settling time, and overshoot. The proposed method exhibits a remarkably low rise time of 0.0318 *s*, indicating its ability to reach a stable output voltage quickly after a disturbance. Similarly, the settling time of 0.0478 *s* for the proposed method suggests its capability to settle down to the desired output voltage within a short duration after a disturbance. Besides, the proposed method shows no overshoot, which is a significant improvement compared to several other methods in the literature. Comparing these results with other reported methods, it's evident that the RW-ARO/PIDD^2-PI approach outperforms many of them in terms of both rise time and settling time while maintaining zero overshoot. This suggests the effectiveness and superiority of the proposed method in enhancing the performance of the AVR system.

7.3. Superiority verification of the RW-ARO-based approach via disturbance rejection and harmonic analysis

7.3.1. Considering external disturbance, noise disturbance and saturation-related nonlinearities

In this study, the performance of the RW-ARO-based approach was also assessed by considering the more real conditions such as measurement noise as a disturbance source and the saturation at the input of the generator as a nonlinear effect in the AVR system. Fig. 12 displays the real model of the AVR system with the stated non-ideal conditions. For the saturation block of Fig. 12, the saturating upper and lower values were chosen to be $+10$ pu and -10 pu, respectively [2].

With regards to measurement noise, a white Gaussian noises with the signal-to-noise ratio (SNR) of 30 *dB* was considered. Besides, an external disturbance of 30% was also introduced to the system at time $t = 1$ *s*. The non-ideal model response of the proposed method considering these cases is presented in Fig. 13. As can be observed from this figure, the proposed method demonstrates a good immunity against noise and disturbance, thus, handles non-ideal cases effectively.

7.3.2. Total harmonic distortion

In this section, we analyze the results of the total harmonic distortion (THD) which is a crucial metric for assessing the quality of an AVR system. Maintaining THD values as low as possible is imperative to ensure the connected equipment remains unaffected by electrical noise and disturbances. In this study, the analysis of THD was conducted utilizing the fast Fourier transform (FFT) tool within the MATLAB/Simulink environment. The fundamental frequency utilized in the system was set to 0.25 Hz.

To gauge the performance of the AVR system, Fig. 14 showcases the output voltage response concerning a reference sine wave input. Remarkably, the output of the proposed RW-ARO/PIDD^2-PI controller aligns closely with the reference signal, exhibiting minimal distortion and highlighting the effectiveness of the approach.

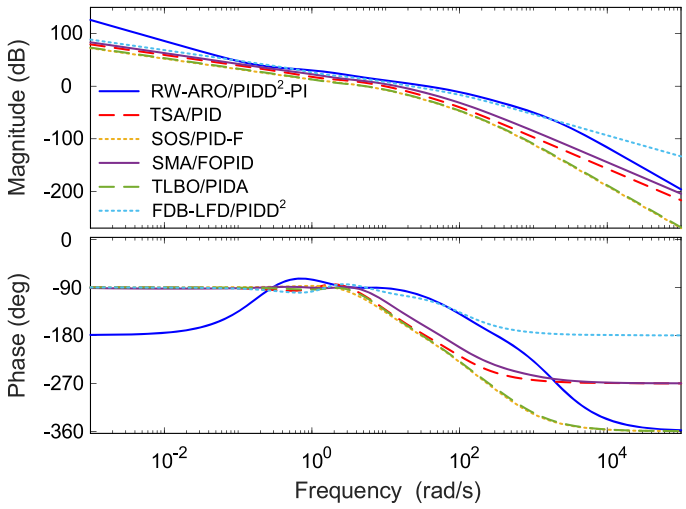

Fig. 11. Comparative Bode plots for RW-ARO/PIDD^2-PI and other recent reported approaches.

Table 7
Comparative numerical values for time and frequency domains related performance metrics.

Stability metric	RW-ARO/PIDD^2-PI	TSA/PID [58]	SOS/PID-F [59]	SMA/FOPID [60]	TLBO/PIDA [61]	FDB-LFD/PIDD^2 [62]
Rise time (s)	**0.0318**	0.1312	0.2658	0.0875	0.2731	0.0638
Settling time (s)	**0.0478**	0.7577	1.3527	0.4979	1.0668	0.0925
Overshoot (%)	**0**	15.5811	0.0224	15.9979	1.0029	1.7034
Phase margin (°)	**70.6399**	48.6094	66.9107	49.1418	71.1892	**72.0921**
Gain margin (dB)	**28.5713**	19.1608	23.8855	20.1925	23.8899	**Infinite**
Bandwidth (rad/s)	**68.3194**	16.2326	8.6985	23.9141	8.7835	32.4815

Table 8
Comparative time domain performance analysis against reported works in the literature.

Proposed control method	Rise time (s)	Settling time (s)	Overshoot (%)
RW-ARO/PIDD^2-PI (novel method)	**0.0318**	**0.0478**	**0**
ICA/Gray PID [31]	0.2305	0.3193	1.23
EO/FOPID-DN [32]	0.076	0.144	**0**
GA/Fuzzy PID [33]	0.1857	0.2963	1.0407
iRUN/Real PIDD^2 [34]	0.0399	0.0626	**0**
Nonlinear SCA/Sigmoid PID [35]	0.498	0.579	2.2
PSO/FHODFC [36]	0.373	0.685	0.001
WOA/2DOF fractional PI [37]	1.12	1.74	1.17
IABC/LOA-FOPID [38]	0.1373	0.3129	2.3323
MA/PI$^{\lambda 1}$I$^{\lambda 2}$D$^{\mu 1}$D$^{\mu 2}$ [39]	0.0323	0.0500	**0**
h-ASPSO/PID [40]	0.3097	0.4679	1.2476

Fig. 15 presents the plot of THD level against frequency. As shown in this figure, the THD oscillates around a mere 0.13%, signifying a good achievement. This result stands in stark contrast to reported values ranging from 0.5% to 4%, underscoring a substantial improvement achieved through the proposed approach. The analysis of THD underscores the effectiveness of the proposed RW-ARO/PIDD^2-PI controller in mitigating harmonic distortions within the AVR system. By achieving remarkably low THD levels, the proposed approach demonstrates its potential in ensuring the reliability and stability of connected electrical equipment.

8. Conclusion

This study has presented a significant advancement in AVR control, focusing on addressing inherent challenges and introducing pioneering contributions to the field. The central motivation was to enhance AVR performance to ensure a consistent and reliable voltage output, critical for optimal electrical system operation and equipment protection. The core of this innovation lies in the development and application of the RW-ARO within the AVR control framework. The RW-ARO strategy leverages a random walk approach to optimize control parameters, resulting in notable improvements in the efficiency and effectiveness of AVR schemes. The novel cascaded RPIDD^2-PI controller, fine-tuned using RW-ARO, represents a groundbreaking advancement in the realm of AVR systems. Its performance surpasses existing methods, offering superior stability, faster response times, enhanced robustness, and improved energy efficiency. Comparative assessments with established controller approaches reaffirm the unique benefits of the proposed methodology. The new approach consistently exhibits shorter rise times, faster settling times, and minimal overshoot, underscoring its exceptional effectiveness and efficiency in achieving desired system responses. Additionally, Bode plots illustrate that the novel approach consistently achieves higher phase and gain margins, further highlighting its superior performance in the frequency domain. In conclusion, this work marks a significant milestone in the domain of AVR control. The incorporation of innovative optimization techniques and advanced controller configurations leads to substantial improvements in stability, speed, robustness, and efficiency. The introduction of the RW-ARO optimization strategy and the cascaded RPIDD^2-PI controller, fine-tuned using this novel approach, underpin the key contributions of this study. Additional assessment of performance compared to previously reported methods reaffirmed the effectiveness of the proposed approach in automatic voltage regulation. Furthermore, analyses of external disturbance rejection and total harmonic distortion were conducted to showcase the superior suitability of the proposed approach for real-world scenarios. These advancements offer enhanced control capabilities and contribute to the development of more resilient and efficient power systems. The insights and innovations presented in this work lay the foundation for future advancements in AVR system control strategies and power system stability.

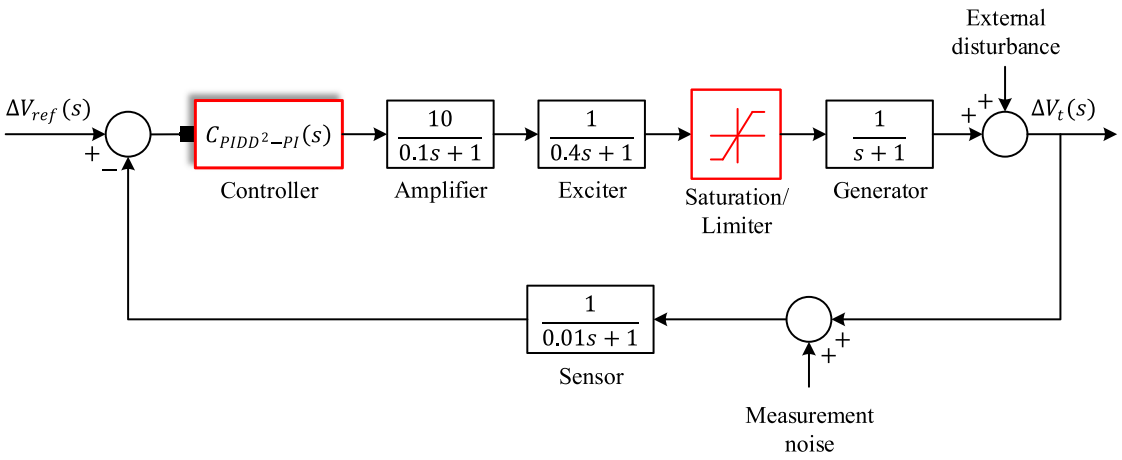

Fig. 12. Real model of the AVR system with non-ideal conditions.

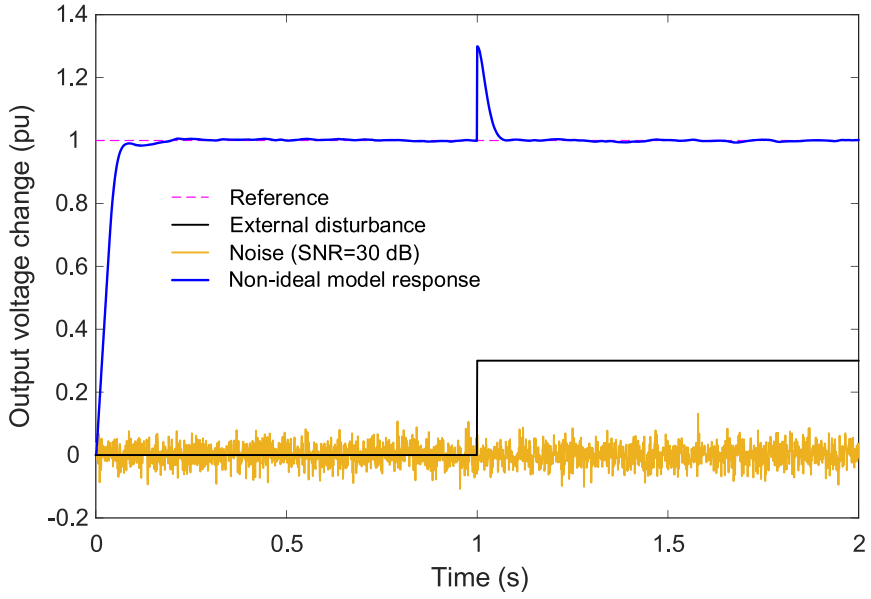

Fig. 13. Non-ideal model response of RW-ARO based cascaded real PIDD^2-PI controlled AVR system with measurement noise and external disturbance.

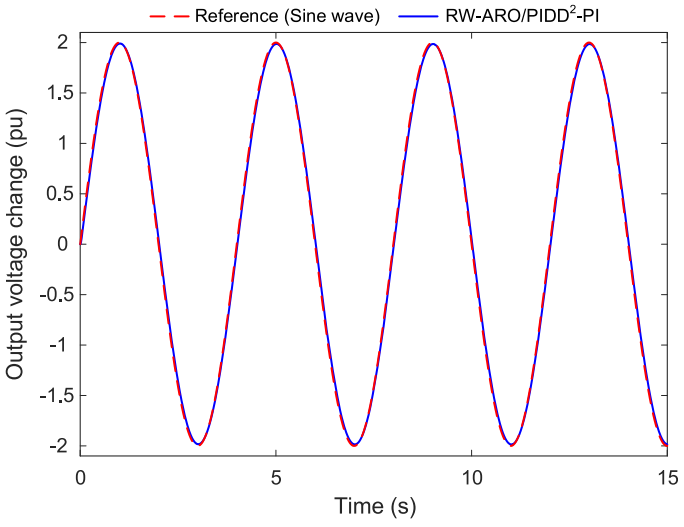

Fig. 14. Output voltage change against a reference sine wave.

Funding statement

The authors received no specific funding for this study.

Ethics approval

This study did not include any human or animal subjects.

CRediT authorship contribution statement

All Authors contributed equally.

Declaration of competing interest

The authors declare that they have no known competing financial interests or personal relationships that could have appeared to influence the work reported in this paper.

Data availability

All the data are available within the paper.

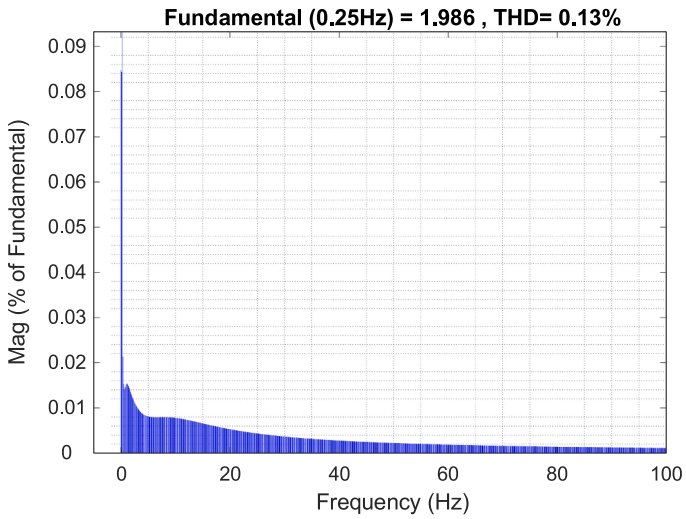

Fig. 15. Total harmonic distortion level against frequency.

References

[1] O. Can, S. Ekinci, D. Izci, Honey badger algorithm for adjustment of FOPID controller adopted in an automatic voltage regulator system, in: 2022 Global Energy Conference (GEC), IEEE, 2022, pp. 262–265, https://doi.org/10.1109/GEC55014.2022.9986660.

[2] D. Izci, L. Abualigah, Ö. Can, C. Andiç, S. Ekinci, Achieving improved stability for automatic voltage regulation with fractional-order PID plus double-derivative controller and mountain gazelle optimizer, Int. J. Dyn. Control (2024), https://doi.org/10.1007/s40435-023-01381-5.

[3] S. Ekinci, D. Izci, R. Abu Zitar, A.R. Alsoud, L. Abualigah, Development of Lévy flight-based reptile search algorithm with local search ability for power systems engineering design problems, Neural Comput. Appl. 34 (2022) 20263–20283, https://doi.org/10.1007/s00521-022-07575-w.

[4] D. Izci, S. Ekinci, A.G. Hussien, Efficient parameter extraction of photovoltaic models with a novel enhanced prairie dog optimization algorithm, Sci. Rep. 14 (2024) 7945, https://doi.org/10.1038/s41598-024-58503-y.

[5] S. Ekinci, Ö. Can, M.Ş. Ayas, D. Izci, M. Salman, M. Rashdan, Automatic generation control of a hybrid PV-reheat thermal power system using RIME algorithm, IEEe Access. 12 (2024) 26919–26930, https://doi.org/10.1109/ACCESS.2024.3367011.

[6] S. Ekinci, D. Izci, A.G. Hussien, Comparative analysis of the hybrid gazelle-Nelder–Mead algorithm for parameter extraction and optimization of solar photovoltaic systems, IET Renew. Power Generat. 18 (2024) 959–978, https://doi.org/10.1049/rpg2.12974.

[7] E. Çelik, IEGQO-AOA: information-exchanged gaussian arithmetic optimization algorithm with quasi-opposition learning, Knowl. Based. Syst. 260 (2023) 110169, https://doi.org/10.1016/j.knosys.2022.110169.

[8] E. Çelik, A powerful variant of symbiotic organisms search algorithm for global optimization, Eng. Appl. Artif. Intell. 87 (2020) 103294, https://doi.org/10.1016/j.engappai.2019.103294.

[9] A.H. Mary, A.H. Miry, M.H. Miry, An optimal robust state feedback controller for the AVR system-based Harris Hawks optimization algorithm, Electric Power Comp. Syst. 48 (2021) 1684–1694, https://doi.org/10.1080/15325008.2021.1908456.

[10] M. Ćalasan, M. Micev, M. Radulović, A.F. Zobaa, H.M. Hasanien, S.H.E. Abdel Aleem, Optimal PID controllers for AVR system considering excitation voltage limitations using hybrid equilibrium optimizer, Machines 9 (2021) 265, https://doi.org/10.3390/machines9110265.

[11] V. Sharma, V. Kumar, R. Naresh, V. Kumar, MPA Optimized Model Predictive Controller for Optimal Control of an AVR System, 2023, pp. 61–70, https://doi.org/10.1007/978-981-19-7524-0_6.

[12] I. Moschos, C. Parisses, A novel optimal PIλDND2N2 controller using coyote optimization algorithm for an AVR system, Eng. Sci. Technol., Int. J. 26 (2022) 100991, https://doi.org/10.1016/j.jestch.2021.04.010.

[13] A.K. Bhullar, R. Kaur, S. Sondhi, A novel fuzzy based weighted aggregation based multi objective function for AVR optimization, J. Intell. Fuzzy Syst. 40 (2021) 9413–9436, https://doi.org/10.3233/JIFS-201911.

[14] M.S. Ayas, A.K. Sahin, A reinforcement learning approach to Automatic Voltage Regulator system, Eng. Appl. Artif. Intell. 121 (2023) 106050, https://doi.org/10.1016/j.engappai.2023.106050.

[15] Ö. Can, C. Andiç, S. Ekinci, D. Izci, Enhancing transient response performance of automatic voltage regulator system by using a novel control design strategy, Electrical Eng. 105 (2023) 1993–2005, https://doi.org/10.1007/s00202-023-01777-8.

[16] R. Mok, M.A. Ahmad, Fast and optimal tuning of fractional order PID controller for AVR system based on memorizable-smoothed functional algorithm, Eng. Sci. Technol., Int. J. 35 (2022) 101264, https://doi.org/10.1016/j.jestch.2022.101264.

[17] M. Ćalasan, M. Micev, Ž. Djurovic, H.M.A. Mageed, Artificial ecosystem-based optimization for optimal tuning of robust PID controllers in AVR systems with limited value of excitation voltage, Int. J. Electric. Eng. Educ. (2020) 002072092094060, https://doi.org/10.1177/0020720920940605.

[18] D. Izci, S. Ekinci, S. Mirjalili, L. Abualigah, An intelligent tuning scheme with a master/slave approach for efficient control of the automatic voltage regulator, Neural Comput. Appl. 35 (2023) 19099–19115, https://doi.org/10.1007/s00521-023-08740-5.

[19] A. Demirören, B. Hekimoğlu, S. Ekinci, S. Kaya, Artificial electric field algorithm for determining controller parameters in AVR system, in: 2019 International Artificial Intelligence and Data Processing Symposium (IDAP), 2019, pp. 1–7, https://doi.org/10.1109/IDAP.2019.8875972.

[20] S. Ekinci, Ö. Can, D. Izci, Controller design for automatic voltage regulator system using modified opposition-based weighted mean of vectors algorithm, Int. J. Modell. Simul. (2023) 1–18, https://doi.org/10.1080/02286203.2023.2274254.

[21] D. Izci, R.M. Rizk-Allah, V. Snášel, S. Ekinci, F.A. Hashim, L. Abualigah, A novel control scheme for automatic voltage regulator using novel modified artificial rabbits optimizer, E-Prime - Adv. Electric. Eng., Electron. Energy 6 (2023) 100325, https://doi.org/10.1016/j.prime.2023.100325.

[22] N.B. Mohamadwasel, Rider optimization algorithm implemented on the AVR control system using MATLAB with FOPID, IOP. Conf. Ser. Mater. Sci. Eng. 928 (2020) 032017, https://doi.org/10.1088/1757-899X/928/3/032017.

[23] E. Çelik, N. Öztürk, A hybrid symbiotic organisms search and simulated annealing technique applied to efficient design of PID controller for automatic voltage regulator, Soft. comput. 22 (2018) 8011–8024, https://doi.org/10.1007/s00500-018-3432-2.

[24] E. Celik, Incorporation of stochastic fractal search algorithm into efficient design of PID controller for an automatic voltage regulator system, Neural Comput. Appl. 30 (2018) 1991–2002, https://doi.org/10.1007/s00521-017-3335-7.

[25] N.D. Chetty, G. Sharma, R. Gandhi, E. Çelik, A novel salp swarm optimization oriented 3-DOF-PIDA controller design for automatic voltage regulator system, IEEe Access. 12 (2024) 20181–20196, https://doi.org/10.1109/ACCESS.2024.3360300.

[26] A.K. Bhullar, R. Kaur, S. Sondhi, Enhanced crow search algorithm for AVR optimization, Soft. comput. 24 (2020) 11957–11987, https://doi.org/10.1007/s00500-019-04640-w.

[27] M.S. Amin, M.A. Attia, A.K. Khamees, S.F. Mekhamer, H. Kotb, K.M. AboRas, A. Yousef, Development of AVR controller performance using exponential distribution and transit search optimization techniques, Front. Energy Res. 12 (2024), https://doi.org/10.3389/fenrg.2024.1356978.

[28] N.I. Smirnov, V.R. Sabanin, A.I. Repin, Sensitivity and robust tuning of PID controllers with real differentiation, Thermal Engineering 54 (2007) 777–785, https://doi.org/10.1134/S0040601507100035.

[29] D. Izci, S. Ekinci, A novel improved version of hunger games search algorithm for function optimization and efficient controller design of buck converter system, E-Prime - Adv. Electric. Eng., Electron. Energy 2 (2022) 100039, https://doi.org/10.1016/j.prime.2022.100039.

[30] D. Izci, S. Ekinci, H.L. Zeynelgil, Controlling an automatic voltage regulator using a novel Harris hawks and simulated annealing optimization technique, Adv. Control Appl. 6 (2024) e121, https://doi.org/10.1002/adc2.121.

[31] Y. Tang, L. Zhao, Z. Han, X. Bi, X. Guan, Optimal gray PID controller design for automatic voltage regulator system via imperialist competitive algorithm, Int. J. Mach. Learn. Cybern. 7 (2016) 229–240, https://doi.org/10.1007/s13042-015-0431-9.

[32] N. Paliwal, L. Srivastava, M. Pandit, Equilibrium optimizer tuned novel FOPID-DN controller for automatic voltage regulator system, Int. Trans. Electric. Energy Syst. 31 (2021) e12930, https://doi.org/10.1002/2050-7038.12930.

[33] T. Dogruer, M.S. Can, Design and robustness analysis of fuzzy PID controller for automatic voltage regulator system using genetic algorithm, Trans. Inst. Measur. Control 44 (2022) 1862–1873, https://doi.org/10.1177/01423312211066758.

[34] D. Izci, S. Ekinci, An improved RUN optimizer based real PID plus second-order derivative controller design as a novel method to enhance transient response and robustness of an automatic voltage regulator, E-Prime - Adv. Electric. Eng., Electron. Energy 2 (2022) 100071, https://doi.org/10.1016/j.prime.2022.100071.
[35] M.H. Suid, M.A. Ahmad, Optimal tuning of sigmoid PID controller using nonlinear sine cosine algorithm for the automatic voltage regulator system, ISA Trans. 128 (2022) 265–286, https://doi.org/10.1016/j.isatra.2021.11.037.
[36] M.S. Ayas, Design of an optimized fractional high-order differential feedback controller for an AVR system, Electric. Eng. 101 (2019) 1221–1233, https://doi.org/10.1007/s00202-019-00842-5.
[37] V. Padiachy, U. Mehta, S. Azid, S. Prasad, R. Kumar, Two degree of freedom fractional PI scheme for automatic voltage regulation, Eng. Sci. Technol., Int. J. 30 (2022) 101046, https://doi.org/10.1016/j.jestch.2021.08.003.
[38] A. Idir, L. Canale, Y. Bensafia, K. Khettab, Design and robust performance analysis of low-order approximation of fractional PID controller based on an iabc algorithm for an automatic voltage regulator system, Energies. (Basel) 15 (2022) 8973, https://doi.org/10.3390/en15238973.
[39] B. Çavdar, E. Şahin, Ö. Akyazı, F.M. Nuroğlu, A novel optimal PIλ1Iλ2Dμ1Dμ2 controller using mayfly optimization algorithm for automatic voltage regulator system, Neural Comput. Appl. 35 (2023) 19899–19918, https://doi.org/10.1007/s00521-023-08834-0.
[40] D. Izci, S. Ekinci, A.G. Hussien, Effective PID controller design using a novel hybrid algorithm for high order systems, PLoS. One 18 (2023) e0286060, https://doi.org/10.1371/journal.pone.0286060.
[41] B. Çavdar, E. Şahin, E. Sesli, On the assessment of meta-heuristic algorithms for automatic voltage regulator system controller design: a standardization process, Electric. Eng. (2024), https://doi.org/10.1007/s00202-024-02314-x.
[42] D. Izci, S. Ekinci, Comparative performance analysis of slime mould algorithm for efficient design of proportional–integral–derivative controller, Electrica 21 (2021) 151–159, https://doi.org/10.5152/electrica.2021.20077.
[43] V.K. Munagala, R.K. Jatoth, Improved fractional PIλDμ controller for AVR system using Chaotic Black Widow algorithm, Comput. Electric. Eng. 97 (2022) 107600, https://doi.org/10.1016/j.compeleceng.2021.107600.
[44] S. Alghamdi, H.F. Sindi, M. Rawa, A.A. Alhussainy, M. Calasan, M. Micev, Z.M. Ali, S.H.E. Abdel Aleem, Optimal PID controllers for AVR systems using hybrid simulated annealing and gorilla troops optimization, Fractal Fractional 6 (2022) 682, https://doi.org/10.3390/fractalfract6110682.
[45] S. Saat, M.R. Ghazali, M.A. Ahmad, N.M.Z.A. Mustapha, M.Z.M. Tumari, An implementation of brain emotional learning based intelligent controller for AVR system, in: 2023 IEEE International Conference on Automatic Control and Intelligent Systems (I2CACIS), IEEE, 2023, pp. 60–64, https://doi.org/10.1109/I2CACIS57635.2023.10193647.
[46] J. Bhookya, R.K. Jatoth, Optimal FOPID/PID controller parameters tuning for the AVR system based on sine–cosine-algorithm, Evol. Intell. 12 (2019) 725–733, https://doi.org/10.1007/s12065-019-00290-x.
[47] M. Micev, M. Ćalasan, D. Oliva, Fractional order PID controller design for an AVR system using chaotic yellow saddle goatfish algorithm, Mathematics 8 (2020) 1182, https://doi.org/10.3390/math8071182.
[48] S. Ekinci, H. Çetin, D. Izci, E. Köse, A novel balanced arithmetic optimization algorithm-optimized controller for enhanced voltage regulation, Mathematics 11 (2023) 4810, https://doi.org/10.3390/math11234810.
[49] S. Ekinci, V. Snášel, R.M. Rizk-Allah, D. Izci, M. Salman, A.A.F. Youssef, Optimizing AVR system performance via a novel cascaded RPIDD2-FOPI controller and QWGBO approach, PLoS. One 19 (2024) e0299009, https://doi.org/10.1371/journal.pone.0299009.
[50] D. Izci, S. Ekinci, S. Mirjalili, Optimal PID plus second-order derivative controller design for AVR system using a modified Runge Kutta optimizer and Bode's ideal reference model, Int. J. Dyn. Control 11 (2023) 1247–1264, https://doi.org/10.1007/s40435-022-01046-9.
[51] L. Wang, Q. Cao, Z. Zhang, S. Mirjalili, W. Zhao, Artificial rabbits optimization: A new bio-inspired meta-heuristic algorithm for solving engineering optimization problems, Eng. Appl. Artif. Intell. 114 (2022) 105082, https://doi.org/10.1016/j.engappai.2022.105082.
[52] X.-S. Yang, T.O. Ting, M. Karamanoglu, Random Walks, Lévy Flights, Markov Chains and Metaheuristic Optimization, 2013, pp. 1055–1064, https://doi.org/10.1007/978-94-007-6516-0_116.
[53] S. Ekinci, D. Izci, M. Kayri, An effective controller design approach for magnetic levitation system using novel improved manta ray foraging optimization, Arab. J. Sci. Eng. 47 (2022) 9673–9694, https://doi.org/10.1007/s13369-021-06321-z.
[54] M. Micev, M. Ćalasan, D. Oliva, Design and robustness analysis of an automatic voltage regulator system controller by using equilibrium optimizer algorithm, Comput. Electric. Eng. 89 (2021) 106930, https://doi.org/10.1016/j.compeleceng.2020.106930.
[55] R. Storn, K. Price, Differential evolution - a simple and efficient heuristic for global optimization over continuous spaces, J. Global Optimiz. 11 (1997) 341–359, https://doi.org/10.1023/A:1008202821328.
[56] E. Rashedi, H. Nezamabadi-pour, S. Saryazdi, GSA: a gravitational search algorithm, Inf. Sci. (N Y) 179 (2009) 2232–2248, https://doi.org/10.1016/j.ins.2009.03.004.
[57] R. Poli, J. Kennedy, T. Blackwell, Particle swarm optimization, Swarm Intell. 1 (2007) 33–57, https://doi.org/10.1007/s11721-007-0002-0.
[58] E. Kose, Optimal control of AVR system with tree seed algorithm-based PID controller, IEEe Access. 8 (2020) 89457–89467, https://doi.org/10.1109/ACCESS.2020.2993628.
[59] B. Ozgenc, M.S. Ayas, I.H. Altas, Performance improvement of an AVR system by symbiotic organism search algorithm-based PID-F controller, Neural Comput. Appl. 34 (2022) 7899–7908, https://doi.org/10.1007/s00521-022-06892-4.
[60] D. Izci, S. Ekinci, H.L. Zeynelgil, J. Hedley, Fractional order PID design based on novel improved slime mould algorithm, Electric Power Comp. Syst. 49 (2021) 901–918, https://doi.org/10.1080/15325008.2022.2049650.
[61] A.M. Mosaad, M.A. Attia, A.Y. Abdelaziz, Comparative performance analysis of AVR controllers using modern optimization techniques, Electric Power Comp. Syst. 46 (2018) 2117–2130, https://doi.org/10.1080/15325008.2018.1532471.
[62] H. Bakir, U. Guvenc, H. Tolga Kahraman, S. Duman, Improved Lévy flight distribution algorithm with FDB-based guiding mechanism for AVR system optimal design, Comput. Ind. Eng. 168 (2022) 108032, https://doi.org/10.1016/j.cie.2022.108032.
[63] Y. Yin, Q. Tu, X. Chen, Enhanced Salp Swarm Algorithm based on random walk and its application to training feedforward neural networks, Soft. comput. 24 (2020) 14791–14807, https://doi.org/10.1007/s00500-020-04832-9.
[64] S. Gupta, K. Deep, A novel random walk grey wolf optimizer, Swarm. Evol. Comput. 44 (2019) 101–112, https://doi.org/10.1016/j.swevo.2018.01.001.
[65] D. Izci, S. Ekinci, E. Eker, A. Dundar, Assessment of slime mould algorithm based real PID plus second-order derivative controller for magnetic levitation system, in: 2021 5th International Symposium on Multidisciplinary Studies and Innovative Technologies (ISMSIT), IEEE, 2021, pp. 6–10, https://doi.org/10.1109/ISMSIT52890.2021.9604620.
[66] B. Hekimoglu, Optimal tuning of fractional order PID controller for DC motor speed control via chaotic atom search optimization algorithm, IEEe Access. 7 (2019) 38100–38114, https://doi.org/10.1109/ACCESS.2019.2905961.
[67] D. Izci, R.M. Rizk-Allah, V. Snášel, S. Ekinci, H. Migdady, M.Sh. Daoud, M. Altalhi, L. Abualigah, Refined sinh cosh optimizer tuned controller design for enhanced stability of automatic voltage regulation, Electric. Eng. (2024), https://doi.org/10.1007/s00202-024-02344-5.
[68] D. Izci, Design and application of an optimally tuned PID controller for DC motor speed regulation via a novel hybrid Lévy flight distribution and Nelder–Mead algorithm, Trans. Inst. Measur. Control 43 (2021) 3195–3211, https://doi.org/10.1177/01423312211019633.
[69] A. Sikander, P. Thakur, R.C. Bansal, S. Rajasekar, A novel technique to design cuckoo search based FOPID controller for AVR in power systems, Comput. Electric. Eng. 70 (2018) 261–274, https://doi.org/10.1016/j.compeleceng.2017.07.005.
[70] A. Tabak, Maiden application of fractional order PID plus second order derivative controller in automatic voltage regulator, Int. Trans. Electric. Energy Syst. 31 (2021), https://doi.org/10.1002/2050-7038.13211.
[71] S. Panda, B.K. Sahu, P.K. Mohanty, Design and performance analysis of PID controller for an automatic voltage regulator system using simplified particle swarm optimization, J. Franklin. Inst. 349 (2012) 2609–2625, https://doi.org/10.1016/j.jfranklin.2012.06.008.
[72] S. Ekinci, A. Demiroren, H. Zeynelgil, B. Hekimoğlu, An opposition-based atom search optimization algorithm for automatic voltage regulator system, J. Faculty Eng. Architect. Gazi Univ. 35 (2020) 1141–1158, https://doi.org/10.17341/gazimmfd.598576.

Erdal Eker was born in Van, Turkey in 1973. He was graduated from Van Yuzuncu Yil University, Turkey, in Mathematics. He received his Msc from Ataturk University, Turkey, in Applied Mathematics and received his PhD from Yuzuncu Yil University in Statistics. He is currently an instructor at Mus Alparslan University, Turkey.

Davut Izci received the B.Sc. degree in electrical and electronic engineering from Dicle University, Turkey, and the M.Sc. and Ph.D. degrees in mechatronics and microsystems from Newcastle University, England, U.K. He is currently an Associate Professor working on optimization, control system design, sensing applications, energy harvesting, microsystems development and applications of metaheuristic optimization techniques to different control systems, and real-world engineering problems. He has published more than 100 articles in prestigious international journals. He is also a member of the editorial board in e-prime journal (Elsevier) and serves as a reviewer in several top tier journals in the field of metaheuristics, artificial intelligence, and control systems. He is recognized as one of the world's top 2% scientists by Elsevier and Stanford University.

Serdar Ekinci received his BSc degree in Control Engineering, and his MSc and PhD degrees in Electrical Engineering all from Istanbul Technical University (ITU), in 2007, 2010 and 2015, respectively. He is currently an Associate Professor working in Department of Computer Engineering at Batman University, Turkey. His areas of interest are electrical power systems, stability, control technology and the applications of metaheuristic optimization algorithms to various control systems.

Hazem Migdady is a professor at the Oman College of Management and Technology, Barka, Sultanate of Oman. He currently serves as the dean of the Oman College. His main research interests are Application Programming Interfaces, Artificial Intelligence, Artificial Intelligence Systems, Artificial Intelligence Techniques, Banking Systems, Bidding, Black Boxes, Box Tests, Business Courses, Collection Systems, Composite Reliability, Composite Reliability Values, Computer Vision, Convolution Matrix, and Convolutional Neural networks.

Raed Abu Zitar is a Professor with the Sorbonne Centre for Artificial Intelligence (SCAI Abu Dhabi), Sorbonne University Abu Dhabi. His main research interests include artificial intelligence, machine learning, pattern recognition, artificial intelligence in software engineering, robotics, computer networks modeling, corpuses development, languages dictionaries, emotions modeling, emotional agents, genetic algorithms, neural networks, intelligent control, scheduling methods, speech recognition, evolutionary based applications, and fuzzy logic.

Laith Abualigah is an Associate Professor at Prince Hussein Bin Abdullah College for Information Technology, Al-Bayt University, Jordan. He is also a distinguished researcher at the School of Computer Science, Universiti Sains Malaysia, Malaysia. He received his first degree from Al-Albayt University, Computer Information System, Jordan, in 2011. He earned a Master's degree from Al-Albayt University, Computer Science, Jordan, in 2014. He received a Ph.D. degree from the School of Computer Science at Universiti Sains Malaysia (USM), Malaysia, in 2018. According to the report published by Clarivate, I'm one of the Highly Cited Researchers in 2021 and 2022 and the 1% influential Researchers, which depicts the 6938 top scientists in the world. And I'm the first researcher in the domain of Computer Science in Jordan for 2021. According to the report published by Stanford University in 2020, Abualigah is one of the 2 % influential scholars, which depicts the 100,000 top scientists in the world. Abualigah has published more than 250 journal papers and books, which collectively have been cited more than 12,500 times (H-index = 45). His-main research interests focus on Arithmetic Optimization Algorithm (AOA), Bio-inspired Computing, Nature-inspired Computing, Swarm Intelligence, Artificial Intelligence, Meta-heuristic Modeling, and Optimization Algorithms, Evolutionary Computations, Information Retrieval, Text clustering, Feature Selection, Combinatorial Problems, Optimization, Advanced Machine Learning, Big data, and Natural Language Processing. Abualigah currently serves as an associate editor of the Journal of Cluster Computing (Springer), the Journal of Soft Computing (Springer), and the Journal of Engineering Applications of Artificial Intelligence (Elsevier).